



HAL
open science

Medial prefrontal cortex pathology in schizophrenia as revealed by convergent findings from multimodal imaging

Edith Pomarol-Clotet, Erick Canales Rodriguez, Raymond Salvador, Salvador Sarro, Jesus Gomar, Fidel Vila, Jordi Ortiz-Gil, Yasser Iturria Medina, Antoni Capdevila, Peter Mckenna

► To cite this version:

Edith Pomarol-Clotet, Erick Canales Rodriguez, Raymond Salvador, Salvador Sarro, Jesus Gomar, et al.. Medial prefrontal cortex pathology in schizophrenia as revealed by convergent findings from multimodal imaging. *Molecular Psychiatry*, 2010, n/a (n/a), pp.n/a-n/a. 10.1038/mp.2009.146 . hal-00499663

HAL Id: hal-00499663

<https://hal.science/hal-00499663>

Submitted on 12 Jul 2010

HAL is a multi-disciplinary open access archive for the deposit and dissemination of scientific research documents, whether they are published or not. The documents may come from teaching and research institutions in France or abroad, or from public or private research centers.

L'archive ouverte pluridisciplinaire **HAL**, est destinée au dépôt et à la diffusion de documents scientifiques de niveau recherche, publiés ou non, émanant des établissements d'enseignement et de recherche français ou étrangers, des laboratoires publics ou privés.

Medial prefrontal cortex pathology in schizophrenia as revealed by convergent findings from multimodal imaging

Edith Pomarol-Clotet^{1,2}, Erick Jorge Canales-Rodriguez^{1,2}, Raymond Salvador^{1,2}, Salvador Sarró^{1,2,3}, Jesús J. Gomar^{1,2}, Fidel Vila⁴, Jordi Ortiz-Gil^{1,2}, Yasser Iturria-Medina⁵, Antoni Capdevila⁴, Peter J. McKenna^{1,2}

¹Benito Menni Complex Assistencial en Salut Mental, Barcelona

²CIBERSAM, Spain

³Psychiatry and Clinical Psychology Programme, Universitat Autònoma de Barcelona, Spain

⁴Fundació Sant Joan de Déu, Barcelona, Spain

⁵Neuroimaging Department, Cuban Neuroscience Center, Havana, Cuba.

Address for correspondence: Dr Edith Pomarol-Clotet, Benito Menni CASM.
Germanes Hospitalàries del Sagrat Cor de Jesús, C/ Dr Antoni Pujadas 38-C, 08830 -
Sant Boi de Llobregat (BARCELONA).
Email: edith.pomarol@gmail.com

Conflict of interest: None of the authors declare any conflicts of interest.

Word count: 3916

Acknowledgments: Supported by the Instituto de Salud Carlos III, Centro de Investigación en Red de Salud Mental, CIBERSAM. Edith Pomarol-Clotet was supported by a Marie Curie European Reintegration Grant (MERG-CT-2004-511069). This work will be included as part of Salvador Sarró's doctoral thesis in the Universitat Autònoma de Barcelona.

Abstract

Neuroimaging studies have found evidence of altered brain structure and function in schizophrenia, but have had complex findings regarding the localisation of abnormality. We applied multimodal imaging (voxel-based morphometry (VBM), fMRI and diffusion tensor imaging (DTI) combined with tractography) to 32 chronic schizophrenic patients and matched healthy controls. At a conservative threshold of $p=0.01$ corrected, structural and functional imaging revealed overlapping regions of abnormality in the medial frontal cortex. DTI found that white matter abnormality predominated in the anterior corpus callosum, and analysis of the anatomical connectivity of representative seed regions again implicated fibres projecting to the medial frontal cortex. There was also evidence of convergent abnormality in the dorsolateral prefrontal cortex, although here the laterality was less consistent across techniques. The medial frontal region identified by these three imaging techniques corresponds to the anterior midline node of the default mode network, a brain system which is believed to support internally directed thought, a state of watchfulness, and/or the maintenance of one's sense of self, and which is of considerable current interest in neuropsychiatric disorders.

Among the many lines of investigation undertaken to characterise the brain pathology of schizophrenia, one of the most productive has been neuroimaging. Early studies using CT established beyond doubt that there is lateral ventricular enlargement in the disorder¹, and MRI studies have shown that this is coupled with a small degree of brain tissue volume reduction, of around 2%². MRI studies have also suggested that brain volume loss in schizophrenia, while widespread, is not homogeneous, but is instead most pronounced in medial temporal lobe structures² and in the grey matter of the superior temporal cortex³. Recent studies using voxel-based morphometry (VBM), which identifies clusters of difference between groups of subjects in an unbiased way without the necessity of preselecting regions of interest, have confirmed that cortical grey matter volume reductions are prominent in parts of the temporal lobe cortex⁴. However, these studies have also found evidence of volume reductions in other areas, including the anterior cingulate cortex, the insular cortex, the left middle frontal gyrus and the postcentral gyrus⁵.

While structural imaging has implicated a variety of brain regions in schizophrenia, the emphasis in functional imaging studies has been and continues to be on the frontal lobes. The original functional imaging finding of hypofrontality, while not consistently replicated, has been supported by meta-analysis both at rest and under conditions of neuropsychological task activation⁶. At the same time, it is increasingly clear that the prefrontal cortex dysfunction in schizophrenia goes beyond any simple concept of hypofunction. Thus, rather than hypofrontality, a number of studies have found evidence of increased activation in the prefrontal cortex (PFC) during performance of working memory tasks⁷⁻¹⁰. This 'hyperfrontality' has been found in dorsolateral and ventral prefrontal regions, and whether it is seen appears to depend on the nature of the

task used, and how well the patients perform it⁹⁻¹³. Complicating matters further, two recent studies have found that schizophrenic patients show a failure of task-related de-activation in the medial frontal cortex^{14, 15}. This medial frontal area corresponds to part of the so-called default mode network, a series of interconnected regions that are highly active at rest but which de-activate during performance of a wide range of cognitive tasks^{16, 17}.

A third imaging technique which is increasingly being applied to schizophrenia is diffusion tensor imaging (DTI). This indexes white matter abnormality by means of decreased fractional anisotropy (FA)¹⁸; tractography algorithms can also be employed to identify which particular tracts are affected. Over 20 studies have indicated that schizophrenia is associated with decreased FA, particularly in white matter tracts connecting temporal and prefrontal regions. However, to date there is a lack of convergence in the findings, and the majority of studies have used a region-of-interest (ROI) approach rather than whole-brain-based examination^{19, 20}.

It has been suggested that further understanding of brain pathology in schizophrenia will depend on integration of findings from voxel-based structural techniques with those from functional imaging and white matter tractography using DTI^{21, 22}. To date, however, relatively few such ‘multimodal’ imaging studies have been carried out, and these have either employed only two imaging techniques¹⁹⁻²¹ or have focused on discrete brain structures such as the hippocampus and amygdala²²⁻²⁴. In this study we report, for the first time, use of a whole brain approach combining all three imaging modalities, in order to determine what, if any, common sites of pathology they identify in the disorder.

Method

Subjects

The patient sample consisted of 32 schizophrenic patients recruited from two hospitals. They all met DSM-IV criteria for schizophrenia, based on interview plus review of clinical history. Patients were excluded if: a) they were younger than 18 or older than 65, b) had a history of brain trauma or neurological disease, and c) had shown alcohol/substance abuse within 12 months prior to participation. Twenty-seven were inpatients and 5 were living outside the hospital with relatives or in supported accommodation. They all had chronic illnesses (range 5-39 years), were symptomatic (mean PANSS score 71.97 ± 17.01) and had on average moderately severe illness (Global Assessment of Function [GAF] score = 44.03 ± 10.89). They were all scanned when in relatively stable condition (ie outside any period of acute relapse). All were taking neuroleptic medication (clozapine N=7, other atypicals N=10, typical neuroleptics N=3, combined typical and atypical treatment N=12). fMRI findings on this sample have previously been described by Pomarol-Clotet et al¹⁴.

The controls consisted of 32 healthy individuals selected to be age- and sex-matched to the patients and met the same exclusion criteria. Subjects were recruited from non-medical staff working in the hospital, their relatives and acquaintances, plus from independent sources in the community. They were questioned and excluded if they reported a history of mental illness and/or treatment with psychotropic medication. Written informed consent was obtained from all participants. The study was approved by the local hospital ethics committee.

Procedure

All subjects underwent structural and functional MRI scanning in a single session, using the same 1.5 Tesla GE Signa scanner (General Electric Medical Systems, Milwaukee, Wis) located at the Sant Joan de Déu Hospital in Barcelona (Spain).

Structural imaging: High resolution structural T1 MRI data were acquired with the following acquisition parameters: Matrix size 512x512; 180 contiguous axial slices; voxel resolution 0.47x0.47x1 mm³; echo (TE), repetition (TR) and inversion (TI) times, (TE/TR/TI) = 3.93 ms/2000 ms/710 ms respectively; flip angle 15 degrees.

Structural data were analysed with FSL-VBM, an optimized voxel-based morphometry style analysis^{29,30} carried out with FSL tools²⁵; this yields a measure of difference in local grey matter volume. In a first step, structural images were brain-extracted using BET²⁶. Next, tissue-type segmentation was carried out and the resulting grey-matter partial volume images were aligned to the MNI152 standard space using the FSL tools FLIRT and FNIRT. The resulting images were averaged to create a study-specific template, to which the native grey matter images were non-linearly re-registered. These images were modulated (to correct for local expansion or contraction) by dividing by the Jacobian of the warp field, and they were later smoothed with an isotropic Gaussian kernel with a sigma of 4 mm. Finally, group comparisons between patients and controls were carried out with permutation-based non-parametric tests. These were made with the *randomise* function implemented in FSL, using the recently developed threshold free cluster enhancement method (TFCE), for proper statistical inference of spatially distributed patterns²⁷.

fMRI: The paradigm used has been described in Pomarol et al¹⁴. Scanning was carried out while participants performed a sequential-letter version of the n-back task²⁸. Two levels of memory load (1-back and 2-back) were presented in a blocked design manner. Each block consisted of 24 letters which were shown every 2 seconds (1 s on, 1 s off) and all blocks contained 5 repetitions (1-back and 2-back depending on the block) located randomly within block. Individuals had to detect them and inform by pressing a button. Four 1-back and four 2-back blocks were presented in an interleaved way, and between them, a baseline stimulus (an asterisk flashing with the same frequency as the letters) was always presented for 16 seconds. In order to identify which task had to be performed, characters were shown in green in 1-back blocks and in red in the 2-back blocks. All participants first went through a training session, outside the scanner.

In each individual scanning session 266 volumes were acquired. A gradient echo echo-planar (EPI) sequence depicting the blood-oxygenation-level-dependent (BOLD) contrast was used. Each volume contained 16 axial planes acquired with the following parameters: TR = 2000 ms, TE = 20 ms, flip angle = 70 degrees, section thickness = 7 mm, section skip = .7 mm, in-plane resolution = 3 x 3 mm². The first 10 volumes were discarded to avoid T1 saturation effects.

fMRI image analyses were performed with the FEAT module, included in FSL software³⁰. At a first level, images were corrected for movement, were coregistered to a common stereotaxic space (Montreal Neurologic Institute template), and were spatially smoothed with a Gaussian filter (FWHM = 5 mm). To minimise unwanted movement related effects, individuals with an estimated maximum absolute movement over 3.0 mm, or an average absolute movement higher than 3 mm were discarded from the

study. Finally, group comparisons between patients and controls were performed using the same FEAT module, by means of mixed-effects GLM models²⁹. A z-threshold of 2.3 (the default in FSL) was used to generate the initial set of clusters. FEAT uses Gaussian Random Field theory to properly account for the spatially distributed patterns when performing statistical tests.

DTI: Whole brain diffusion-weighted images were recorded along 25 gradient directions using three different *b*-values (500, 750 and 1000 s/mm²) together with three unweighted (*b* = 0) images (78 images in total). For each image we used the following parameters: field of view FOV=289x289 mm²; matrix size 128x128; number of slices 28; voxel resolution 1.13x1.13x5 mm³; TE = 107 ms; TR = 8000 ms.

DTI datasets were analyzed with FSL-TBSS³⁰, a Tract-Based Spatial Statistics analysis carried out with FSL tools. In a first step, FA images were created by fitting a tensor model to the raw diffusion data using FDT, and then brain-extracted using BET²⁶. All subjects' FA data were then aligned into a common space using the nonlinear registration tool FNIRT [J.L.R. Andersson, M. Jenkinson and S. Smith. Non-linear optimisation: FMRIB technical report TR07JA1 from www.fmrib.ox.ac.uk/analysis/techrep; J.L.R. Andersson, M. Jenkinson and S. Smith. Non-linear registration, aka Spatial normalisation: FMRIB technical report TR07JA2 from www.fmrib.ox.ac.uk/analysis/techrep], which uses a b-spline representation of the registration warp field³¹. Next, the mean FA image was created and thinned to create a mean FA skeleton which represents the centres of all tracts common to the group. Each subject's aligned FA data was then projected onto this skeleton. As in the VBM analysis, group comparisons between patients and controls were performed using the

randomise function implemented in FSL, which carries out permutation based, non parametric comparisons.

Additionally, the output from the DTI analysis was used to explore potential differences in white matter structural connectivity. For this we used the voxel-based methodology described by Iturria-Medina et al^{34,35}, which uses Dijkstra's graph theory algorithm to find the most probable route of connection between any pairs of voxels in the brain. First, the statistical map resulting from TBSS was automatically partitioned into non-overlapping clusters. Next, four of these clusters were selected as representative ROIs, after considering their central location in each of the significant tracts, and avoiding other clusters containing fibre intersections (which would make the interpretation of results difficult). Every ROI was used separately as a seed mask by an optimized tractography algorithm³², delivering three-dimensional images that quantified the degree of anatomical connection between a particular ROI and each voxel in the brain³³. Finally, all individual maps were aligned into a common space and they were smoothed with an isotropic Gaussian kernel with a sigma of 4 mm. This allowed comparing connectivity patterns between patients and controls using the same permutation-based *randomise* function from FSL.

Statistical thresholds

In the three principal analyses comparing patients and controls, a threshold of $p=0.01$, corrected for multiple comparisons across space, was used. We applied this relatively conservative threshold in order to minimise false positive findings arising from the analysis of several modalities and from different sets of images. Using this threshold on the three main comparisons leads to an overall probability of finding one (or more) false

positives of 0.03. Results applying a corrected $p = 0.05$ in the individual tests are reported in the supplementary online material. However, these results should be treated with caution, as they imply an overall probability of 0.14 for false positives in the three main comparisons.

Results

Demographic findings

Demographic findings are shown in Table 1. The patients and controls were selected to be matched for age and sex. There were also no significant differences between their score on the Word Accentuation Test (TAP), a test designed to estimate IQ (premorbid IQ in the patients) analogous to the National Adult Reading Test (NART) in English³⁴, based on pronunciation of low-frequency Spanish words whose accents are removed³⁵. As typically found in schizophrenia, the patients, however, had a lower current IQ than the controls.

VBM

Due to poor image quality, two individuals (1 control and 1 patient) were excluded from the VBM analyses. At a $p=0.01$, only two areas of the brain showed significant differences in volume between patients and controls (see Figure 1A). One of these was centred in the medial frontal cortex [peak in Brodmann area 32 (BA 32), Talairach (-8, 14, 46), z score=5.95, $p<0.001$], bilaterally including parts of the gyrus rectus, anterior cingulate, medial superior frontal gyrus, and extending posteriorly to the supplementary motor area. The second significant area was located in the right hemisphere, partially covering the dorsolateral prefrontal cortex and extending to inferior frontal cortical

regions and the precentral gyrus with a maximum in BA 44 [Talairach (50, 8, 24), z score=4.7, $p<0.0197$].

[Figure 1 about here]

fMRI

While the 1-back vs baseline contrast did not reveal any significant differences in activation, the 2-back vs baseline contrasts revealed several areas of differential activation between the two groups. The patients showed significantly reduced activation compared to controls in two areas (Figure 1B, shown in blue). One of these areas comprised two distinct but clearly related clusters [cluster1: peak activation in BA 8, Talairach (2, 26, 50), z score=4.35, $p<1.19 \cdot 10^{-7}$; cluster2: peak activation in BA 6, Talairach (-46, -2, 28), z score=4.12, $p<0.00131$]. These clusters included parts of the frontal operculum bilaterally, both precentral gyri and the supplementary motor areas. They also it reached some sections of the right dorsolateral prefrontal cortex and the left basal ganglia. The other area was located in the cerebellum [peak activation in Talairach coordinates (2, -56, -24), z score=5.96, $p<1.91 \cdot 10^{-8}$].

Additionally, patients showed significant failure to de-activate in two clusters (Figure 1B, shown in orange). One of these extended over a large medial frontal area including, bilaterally, the gyrus rectus, the anterior cingulate cortex and parts of the superior medial frontal cortex and related frontomedial structures [peak activation in BA 11, Talairach (-2, 38, -2), z score=4.91, $p<1.78 \cdot 10^{-9}$]. This cluster clearly overlapped with the region of volume reduction identified in the VBM analysis (Figure 1A). The other cluster where there was significant failure to deactivate was smaller, and contained parts

of the hippocampal complex and neighbouring anterior temporal regions with maximum activation in BA 48 [Talairach (46, -8, -12), z score=4.04, $p < 0.000798$].

DTI

Due to excessive movement only 25 patients and 28 controls could be included in this analysis. At $p = 0.01$ corrected, the major FA differences between the patients and controls were found in the corpus callosum [maximum in Talairach space (22, 37, -1), $p < 0.00701$] (see Figure 2A). In particular, alterations were seen in the anterior portion of this structure, extending from below the genu to include the rostral and anterior midbody. This area of significant difference also included the anterior corona radiata bilaterally (visible particularly in the left-hand figure).

A further anomalous region was located posteriorly in the splenium of the corpus callosum on the left, also involving the posterior thalamic radiation (including the optic radiation) and to a lesser extent the posterior corona radiata [maximum at Talairach coordinates (-21, -83, 10), $p < 0.007$].

In order to examine the relationship of the anterior callosal FA differences to the overlapping areas of structural and functional MRI abnormality in the medial prefrontal cortex, we performed a connectivity/tractography analysis (see Methods). For this, four ROIs were selected from an automatic parcellation of all areas with significant differences in FA at $p = 0.01$. ROI#1 corresponded to the genu of the corpus callosum in the midline; ROI#2 and ROI#3 were components of the left and right parts of the body of the corpus callosum anteriorly; ROI#4 was located within the posterior thalamic radiation. In this analysis we first applied a less conservative threshold of 0.05 rather

than the 0.01 used in all other analyses: we expected higher levels of noise inherent to limitations in both the diffusion tensor model³⁶ and the tractography algorithm to reduce the statistical power of the connectivity analyses.

The three anteriorly placed seed regions (ROI#1, ROI#2, ROI#3) showed significant connectivity differences between patients and controls which affected principally a large expanse of the medial frontal cortex (see Figure 2B). Noticeably, there is a clear overlap between these results and areas showing failure to deactivate in fMRI and regions with volume reduction in VBM (Figure 1A and B). The seed placed in the left side of the body of the corpus callosum also showed differential connectivity with the left dorsolateral prefrontal cortex. The fourth seed, located posteriorly in the posterior thalamic radiation, did not result in any differential connectivity between the schizophrenic patients and the controls.

Repeating the analyses at a threshold of 0.01 corrected had similar results, but the area of differential structural connectivity was less extensive. In particular, only the seed region ROI#3 in the right part of the body of the corpus callosum continued to show significant differences between patients and controls. These affected areas very similar to those depicted in the lower panel of Figure 2B, but unilaterally on the right side of the brain.

Discussion

In this study three different whole-brain voxel-based imaging techniques identified the medial prefrontal cortex as a prominent site of abnormality in schizophrenia. This region has not previously been a focus of interest in the disorder, although some post-

mortem studies have noted microstructural abnormalities in the anterior cingulate cortex³⁷, and it is an area where apparent hyperactivation¹², and more recently failure of de-activation^{14, 15} has been found in the disorder (see below). We also found evidence of convergent abnormality in the dorsolateral prefrontal cortex, which is an area of longstanding interest in schizophrenia. Here, however, the laterality was less consistent across techniques.

Our findings differ from two other studies which have applied whole-brain multimodal imaging to schizophrenia^{19, 20}. Calhoun et al¹⁹ examined 15 chronic schizophrenic patients and 15 controls using VBM and fMRI during performance of an auditory oddball task. They used joint independent component analysis (jICA) of both modalities to determine areas of difference between both groups. Significant differences for VBM and fMRI were located in clearly different cortical regions, and there was no anatomical convergence. Lui et al²⁰ carried out VBM on 68 patients with first-episode schizophrenia and 68 controls. Like us, they found a cluster of grey matter volume reduction in the anterior cingulate cortex (although on the right only), along with two other clusters in the right superior and right middle temporal gyri. However, when the authors used these three regions as seeds for a functional connectivity analysis using resting fMRI, no differences between the patients and the controls emerged.

Our findings are also different from those of other studies using single modalities of brain imaging. In particular, we found a considerably less extensive pattern of brain abnormality in the VBM and DTI analyses than in previous studies. On the one hand, this undoubtedly reflects our use of a conservative threshold of $p=0.01$ corrected. Thus, while two recent meta-analyses of VBM studies in schizophrenia^{5, 38} found, like us,

clusters of reduced volume in the medial prefrontal cortex and the dorsolateral prefrontal cortex, these were accompanied by other clusters, notably in the insula/inferior frontal cortex and the medial temporal lobes. Some of these additional areas were also evident in our analysis using a threshold of $p=0.05$ (see supplementary online material).

On the other hand, there are grounds for believing that VBM abnormality in schizophrenia may not be as widespread as originally thought. When the technique was originally introduced in 2000-2001^{39,40}, it utilized a measure of grey matter concentration or density, the proportion of grey matter within a given voxel after spatial normalization of the images. Later, a modulated or ‘optimized’ method became available which gives a more intuitive estimate of grey matter volume. Fornito et al³⁸ meta-analyzed studies using measures of grey matter concentration in schizophrenia and found clusters of significant volume reduction in the medial and lateral frontal cortex, temporal cortex and insula bilaterally. However, meta-analysis of studies using the volume measure resulted in a more restricted pattern of differences: changes in the temporal lobe and insula were no longer seen, and the largest areas of reduced volume were in the medial aspect of the left superior frontal gyrus plus the left orbitofrontal and fusiform regions.

DTI studies of schizophrenia have found evidence of abnormality in many different white matter areas, although these include the corpus callosum^{19,20}, especially in recent studies^{21,41}. Once again, however, there are grounds for believing that the true pattern may be more restrictive: Ellison-Wright and Bullmore⁴² meta-analyzed 15 studies which used a whole brain, voxel-based approach and found that only two locations were

consistently identified across studies. One of these was in the deep white matter of the left frontal lobe, close to the genu of the corpus callosum. The other area was in the left temporal lobe white matter. These areas are strikingly similar to those we found using a threshold of $p=0.01$ corrected.

The linchpin for the convergence of evidence found in our study is the failure of de-activation in the medial frontal cortex, which was equally prominent at thresholds of $p=0.05$ or $p=0.01$. One of the most important functional imaging findings to emerge in recent years has been that prefrontal cortex dysfunction in schizophrenia goes beyond any simple concept of hypofrontality, with a series of studies documenting areas of increased activation ('hyperfrontality') during performance of working memory tasks⁷⁻¹⁰. The leading interpretation of this finding has been that of cortical inefficiency: even when schizophrenic patients are able to perform a cognitive task normally, they have to 'work harder to keep up' with its demands, and this leads to a compensatory brain functional response characterized by greater and/or wider activation of relevant cortical regions than in healthy subjects^{10, 13}. However, a meta-analysis of fMRI studies using the n-back task¹² casts doubts on this interpretation, since a) hyperfrontality was found in the medial prefrontal cortex, different from the dorsolateral and other lateral areas where hypofrontality was seen; and b) this medial frontal area was not activated in the meta-analysis of either patients alone or controls alone. Subsequently, findings from two studies suggest that the hyperfrontality seen in medial frontal cortex in schizophrenia actually represents a failure to de-activate^{14, 15} (because of 'reverse subtraction' from a high baseline, this can result in apparent hyperactivation, see Gusnard and Raichle⁴³).

What is the function of this medial prefrontal area identified by multimodal imaging? As mentioned above, it includes, but is not limited to, the anterior cingulate cortex, an area which has been implicated in mood, attention, emotional regulation, error detection and decision making^{37, 44}. Perhaps more significantly, it corresponds closely to one of the two midline nodes of the default mode network, a system of brain regions which are active at rest but de-activate during performance of a wide range of attention demanding cognitive tasks¹⁶. The default mode network has been proposed to be involved in functions like conceiving the perspectives of others, retrieving autobiographical memories and envisioning the future, processes which can be subsumed under a broad heading of mentation detached from the external world¹⁷. Going further, it has been argued that such functions underlie the experience and maintenance of one's sense of self⁴⁵. A further possibility is that the default mode network underlies a state of 'watchfulness', a passive, low-level monitoring of the external environment for unexpected events in conditions when active attention is relaxed¹⁷. Any and all of these possibilities appear to have scope for explaining the symptoms of schizophrenia.

References

1. Van Horn JD, McManus IC. Ventricular enlargement in schizophrenia. A meta-analysis of studies of the ventricle:brain ratio (VBR). *Br J Psychiatry* 1992; **160**: 687-697.
2. Wright IC, Rabe-Hesketh S, Woodruff PW, David AS, Murray RM, Bullmore ET. Meta-analysis of regional brain volumes in schizophrenia. *Am J Psychiatry* 2000; **157**: 16-25.
3. McCarley RW, Wible CG, Frumin M, Hirayasu Y, Levitt JJ, Fischer IA *et al*. MRI anatomy of schizophrenia. *Biol Psychiatry* 1999; **45**: 1099-1119.
4. Honea R, Crow TJ, Passingham D, Mackay CE. Regional deficits in brain volume in schizophrenia: a meta-analysis of voxel-based morphometry studies. *Am J Psychiatry* 2005; **162**: 2233-2245.

5. Glahn DC, Laird AR, Ellison-Wright I, Thelen SM, Robinson JL, Lancaster JL *et al.* Meta-analysis of gray matter anomalies in schizophrenia: application of anatomic likelihood estimation and network analysis. *Biol Psychiatry* 2008; **64**: 774-781.
6. Hill K, Mann L, Laws KR, Stephenson CM, Nimmo-Smith I, McKenna PJ. Hypofrontality in schizophrenia: a meta-analysis of functional imaging studies. *Acta Psychiatr Scand* 2004; **110**: 243-256.
7. Manoach DS, Press DZ, Thangaraj V, Searl MM, Goff DC, Halpern E *et al.* Schizophrenic subjects activate dorsolateral prefrontal cortex during a working memory task, as measured by fMRI. *Biol Psychiatry* 1999; **45**: 1128-1137.
8. Callicott JH, Bertolino A, Mattay VS, Langheim FJ, Duyn J, Coppola R *et al.* Physiological dysfunction of the dorsolateral prefrontal cortex in schizophrenia revisited. *Cereb Cortex* 2000; **10**: 1078-1092.
9. Tan HY, Suss T, Buckholz JW, Mattay VS, Meyer-Lindenberg A, Egan MF *et al.* Dysfunctional prefrontal regional specialization and compensation in schizophrenia. *Am J Psychiatry* 2006; **163**: 1969-1977.
10. Callicott JH, Mattay VS, Verchinski BA, Marenco S, Egan MF, Weinberger DR. Complexity of prefrontal cortical dysfunction in schizophrenia: more than up or down. *Am J Psychiatry* 2003; **160**: 2209-2215.
11. Manoach DS. Prefrontal cortex dysfunction during working memory performance in schizophrenia: reconciling discrepant findings. *Schizophr Res* 2003; **60**: 285-298.
12. Glahn DC, Ragland JD, Abramoff A, Barrett J, Laird AR, Bearden CE *et al.* Beyond hypofrontality: a quantitative meta-analysis of functional neuroimaging studies of working memory in schizophrenia. *Hum Brain Mapp* 2005; **25**: 60-69.
13. Tan HY, Callicott JH, Weinberger DR. Dysfunctional and compensatory prefrontal cortical systems, genes and the pathogenesis of schizophrenia. *Cereb Cortex* 2007; **17 Suppl 1**: i171-181.
14. Pomarol-Clotet E, Salvador R, Sarro S, Gomar J, Vila F, Martinez A *et al.* Failure to deactivate in the prefrontal cortex in schizophrenia: dysfunction of the default mode network? *Psychol Med* 2008; **38**: 1185-1193.
15. Whitfield-Gabrieli S, Thermenos HW, Milanovic S, Tsuang MT, Faraone SV, McCarley RW *et al.* Hyperactivity and hyperconnectivity of the default network in schizophrenia and in first-degree relatives of persons with schizophrenia. *Proc Natl Acad Sci U S A* 2009; **106**: 1279-1284.
16. Raichle ME, MacLeod AM, Snyder AZ, Powers WJ, Gusnard DA, Shulman GL. A default mode of brain function. *Proc Natl Acad Sci U S A* 2001; **98**: 676-682.

17. Buckner RL, Andrews-Hanna JR, Schacter DL. The brain's default network: anatomy, function, and relevance to disease. *Ann N Y Acad Sci* 2008; **1124**: 1-38.
18. Basser PJ, Pierpaoli C. Microstructural and physiological features of tissues elucidated by quantitative-diffusion-tensor MRI. *J Magn Reson B* 1996; **111**: 209-219.
19. Calhoun VD, Adali T, Giuliani NR, Pekar JJ, Kiehl KA, Pearlson GD. Method for multimodal analysis of independent source differences in schizophrenia: combining gray matter structural and auditory oddball functional data. *Hum Brain Mapp* 2006; **27**: 47-62.
20. Lui S, Deng W, Huang X, Jiang L, Ma X, Chen H *et al.* Association of cerebral deficits with clinical symptoms in antipsychotic-naive first-episode schizophrenia: an optimized voxel-based morphometry and resting state functional connectivity study. *Am J Psychiatry* 2009; **166**: 196-205.
21. Miyata J, Hirao K, Namiki C, Fujiwara H, Shimizu M, Fukuyama H *et al.* Reduced white matter integrity correlated with cortico-subcortical gray matter deficits in schizophrenia. *Schizophr Res* 2009, 111, 78-85.
22. Kalus P, Buri C, Slotboom J, Gralla J, Remonda L, Dierks T *et al.* Volumetry and diffusion tensor imaging of hippocampal subregions in schizophrenia. *Neuroreport* 2004; **15**: 867-871.
23. Kalus P, Slotboom J, Gallinat J, Federspiel A, Gralla J, Remonda L *et al.* New evidence for involvement of the entorhinal region in schizophrenia: a combined MRI volumetric and DTI study. *Neuroimage* 2005; **24**: 1122-1129.
24. Kalus P, Slotboom J, Gallinat J, Wiest R, Ozdoba C, Federspiel A *et al.* The amygdala in schizophrenia: a trimodal magnetic resonance imaging study. *Neurosci Lett* 2005; **375**: 151-156.
25. Smith SM, Jenkinson M, Woolrich MW, Beckmann CF, Behrens TE, Johansen-Berg H *et al.* Advances in functional and structural MR image analysis and implementation as FSL. *Neuroimage* 2004; **23 Suppl 1**: S208-219.
26. Smith SM. Fast robust automated brain extraction. *Hum Brain Mapp* 2002; **17**: 143-155.
27. Smith SM, Nichols TE. Threshold-free cluster enhancement: addressing problems of smoothing, threshold dependence and localisation in cluster inference. *Neuroimage* 2009; **44**: 83-98.
28. Gevins A, Cuttillo B. Spatiotemporal dynamics of component processes in human working memory. *Electroencephalogr Clin Neurophysiol* 1993; **87**: 128-143.

29. Beckmann CF, Jenkinson M, Woolrich MW, Behrens TE, Flitney DE, Devlin JT *et al.* Applying FSL to the FIAC data: model-based and model-free analysis of voice and sentence repetition priming. *Hum Brain Mapp* 2006; **27**: 380-391.
30. Smith SM, Jenkinson M, Johansen-Berg H, Rueckert D, Nichols TE, Mackay CE *et al.* Tract-based spatial statistics: voxelwise analysis of multi-subject diffusion data. *Neuroimage* 2006; **31**: 1487-1505.
31. Rueckert D, Sonoda L, Hayes C, Hill D, Leach M, Hawkes D. Non-rigid registration using free-form deformations: Application to breast MR images. *IEEE Transactions on Medical Imaging* 1999; **18**: 712-721.
32. Iturria-Medina Y, Canales-Rodriguez EJ, Melie-Garcia L, Valdes-Hernandez PA, Martinez-Montes E, Aleman-Gomez Y *et al.* Characterizing brain anatomical connections using diffusion weighted MRI and graph theory. *Neuroimage* 2007; **36**: 645-660.
33. Iturria-Medina Y, Sotero RC, Canales-Rodriguez EJ, Aleman-Gomez Y, Melie-Garcia L. Studying the human brain anatomical network via diffusion-weighted MRI and Graph Theory. *Neuroimage* 2008; **40**: 1064-1076.
34. Nelson HE, Willison JR. *The Revised National Adult Reading Test*. NFER-Nelson: Windsor, Berks, 1991.
35. Del Ser T, Gonzalez-Montalvo JI, Martinez-Espinosa S, Delgado-Villalpalos C, Bermejo F. Estimation of premorbid intelligence in Spanish people with the Word Accentuation Test and its application to the diagnosis of dementia. *Brain Cogn* 1997; **33**: 343-356.
36. Frank LR. Characterization of anisotropy in high angular resolution diffusion-weighted MRI. *Magn Reson Med* 2002; **47**: 1083-1099.
37. Fornito A, Yucel M, Dean B, Wood SJ, Pantelis C. Anatomical Abnormalities of the Anterior Cingulate Cortex in Schizophrenia: Bridging the Gap Between Neuroimaging and Neuropathology. *Schizophr Bull* 2008, 64: 758.765.
38. Fornito A, Yucel M, Patti J, Wood SJ, Pantelis C. Mapping grey matter reductions in schizophrenia: an anatomical likelihood estimation analysis of voxel-based morphometry studies. *Schizophr Res* 2009; **108**: 104-113.
39. Ashburner J, Friston KJ. Voxel-based morphometry--the methods. *Neuroimage* 2000; **11**: 805-821.
40. Good CD, Johnsrude IS, Ashburner J, Henson RN, Friston KJ, Frackowiak RS. A voxel-based morphometric study of ageing in 465 normal adult human brains. *Neuroimage* 2001; **14**: 21-36.
41. Rotarska-Jagiela A, Schonmeyer R, Oertel V, Haenschel C, Vogeley K, Linden DE. The corpus callosum in schizophrenia-volume and connectivity changes affect specific regions. *Neuroimage* 2008; **39**: 1522-1532.

42. Ellison-Wright I, Bullmore E. Meta-analysis of diffusion tensor imaging studies in schizophrenia. *Schizophr Res* 2009; **108**: 3-10.
43. Gusnard DA, Raichle ME. Searching for a baseline: functional imaging and the resting human brain. *Nat Rev Neurosci* 2001; **2**: 685-694.
44. Devinsky O, Morrell MJ, Vogt BA. Contributions of anterior cingulate cortex to behaviour. *Brain* 1995; **118**: 279-306.
45. Gusnard DA. Being a self: considerations from functional imaging. *Conscious Cogn* 2005; **14**: 679-697.

Table 1. Demographic characteristics of patients and controls.

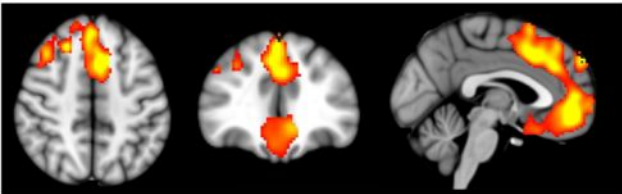
	Patients (n=32)	Controls (n=32)	
Age	41.56±8.79 (28-60)	41.03±11.04 (range 21-59)	P=.83
Sex (M/F)	21/11	21/11	P=1
TAP correct words	21.55±5.58	22.93±4.63	P=.32
Current IQ (WAIS-III)	94.31±9.02 (range 80-110)	100.52±9.10 (range 80-110)	P=.01
Duration of illness (years)	21.79±9.09 (range 5-39)	-	
GAF score	44.03±10.89 (range 22-65)	-	
PANSS score	71.97±17.01 (range 38-116)	-	

Legends for figures

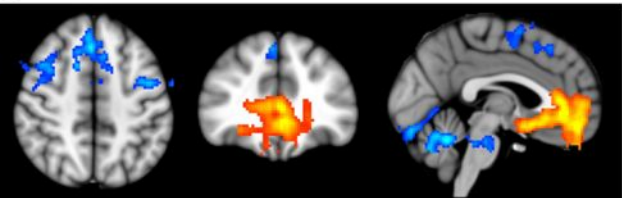
Figure 1. Top panel (A) VBM findings: regions showing significant volume reduction thresholded at $p=0.01$ in the schizophrenic patients are shown in orange. Bottom panel (B) fMRI findings: regions are shown where there were significant differences between patients and controls during performance of the n-back task (2-back vs baseline comparison), thresholded at $p=0.01$. Blue indicates hypoactivation, ie areas where controls activated significantly more than patients. Orange indicates areas where the schizophrenic patients showed failure to de-activate in comparison to controls. The right side of the images represents the left side of the brain.

Figure 2: DTI findings. Top panel (A) shows areas of significant FA reduction in the schizophrenic patients identified using TBSS thresholded at $p=0.01$. Bottom panels (B) show areas of structural connectivity which differed significantly between the schizophrenic patients and controls based on the seed placed in the genu of the corpus callosum (upper, shown in red), and the seeds placed in the body of the corpus callosum, right and left (lower, shown in orange). A threshold of $p=0.05$ corrected was used for this analysis. The right side of the images represents the left side of the brain.

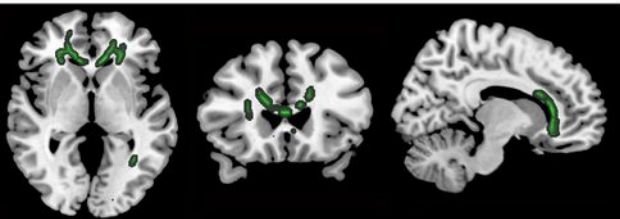
A



B



A



B

